1-1-2015

Enhanced electron lifetime of CdSe/CdS quantum dot (QD) sensitized solar cells using ZnSe core-shell structure with efficient regeneration of quantum dots

Rasin K. Ahmed
Queensland University of Technology

Long Zhao
University of Wollongong, lz796@uowmail.edu.au

Attila J. Mozer
University of Wollongong, attila@uow.edu.au

Geoffrey D. Will
Queensland University of Technology

John M. Bell
Queensland University of Technology

See next page for additional authors

Enhanced electron lifetime of CdSe/CdS quantum dot (QD) sensitized solar cells using ZnSe core-shell structure with efficient regeneration of quantum dots

Abstract

Research on development of efficient passivation materials for high performance and stable quantum dot sensitized solar cells (QDSCs) is highly important. While ZnS is one of the most widely used passivation material in QDSCs, an alternative material based on ZnSe which was deposited on CdS/CdSe/TiO_2 photoanode to form a semi-core/shell structure has been found to be more efficient in terms of reducing electron recombination in QDSCs in this work. It has been found that the solar cell efficiency was improved from 1.86% for ZnSe0 (without coating) to 3.99% using 2 layers of ZnSe coating (ZnSe2) deposited by successive ionic layer adsorption and reaction (SILAR) method. The short circuit current density (J_{sc}) increased nearly 1-fold (from 7.25 mA/cm^2 to13.4 mA/cm^2), and the open circuit voltage (V_{oc}) was enhanced by 100 mV using ZnSe2 passivation layer compared to ZnSe0. Studies on the light harvesting efficiency (η_{LHE}) and the absorbed photon-to-current conversion efficiency (APCE) have revealed that the ZnSe coating layer caused the enhanced η_{LHE} at wavelength beyond 500 nm and a significant increase of the APCE over the spectrum 400-550 nm. A nearly 100% APCE was obtained with ZnSe2, indicating the excellent charge injection and collection process in the device. The investigation on charge transport and recombination of the device has indicated that the enhanced electron collection efficiency and reduced electron recombination should be responsible for the improved J_{sc} and V_{oc} of the QDSCs. The effective electron lifetime of the device with ZnSe2 was nearly 6 times higher than ZnSe0 while the electron diffusion coefficient was largely unaffected by the coating. Study on the regeneration of QDs after photoinduced excitation has indicated that the hole transport from QDs to the reduced species (S^{2-}) in electrolyte was very efficient even when the QDs were coated with a thick ZnSe shell (three layers). For comparison, ZnS coated CdS/CdSe sensitized solar cell with optimum shell thickness was also fabricated, which generated a lower energy conversion efficiency (η = 3.43%) than the ZnSe based QDSC counterpart due to a lower V_{oc} and FF. This study suggests that ZnSe may be a more efficient passivation layer than ZnS, which is attributed to the type II energy band alignment of the core (CdS/CdSe quantum dots) and passivation shell (ZnSe) structure, leading to more efficient electron-hole separation and slower electron recombination.

Keywords

electron, lifetime, cdse, cds, quantum, dot, qd, sensitized, solar, enhanced, cells, structure, znse, core, efficient, shell, regeneration, dots

Disciplines

Engineering | Physical Sciences and Mathematics

Publication Details

Ahmed, R., Zhao, L., Mozer, A. J., Will, G., Bell, J. & Wang, H. (2015). Enhanced electron lifetime of CdSe/CdS quantum dot (QD) sensitized solar cells using ZnSe core-shell structure with efficient regeneration of quantum dots. The Journal of Physical Chemistry C: Energy Conversion and Storage, Optical and Electronic Devices, Interfaces, Nanomaterials, and Hard Matter, 119 (5), 2297-2307.

Authors

Rasin K. Ahmed, Long Zhao, Attila J. Mozer, Geoffrey D. Will, John M. Bell, and Hongxia Wang

Enhanced Electron Lifetime of CdSe/CdS Quantum Dots (QDs) -Sensitized Solar Cells Using ZnSe Core-Shell Structure with Efficient Regeneration of QDs

Rasin Ahmed[†], *Long Zhao*[§], *Attila J. Mozer*[§], *Geoffrey Will*[†], *John Bell*[†] *and Hongxia Wang*[†*]

[†]School of Chemistry, Physics and Mechanical Engineering, Queensland University of Technology, QLD 4001, Australia

[§] Intelligent Polymer Research Institute and ARC Centre of Excellence for Electromaterials Science, University of Wollongong, NSW 2522, Australia

Corresponding Author

[*] Tel: +61 7 3138 1984; Email: hx.wang@qut.edu.au;

KEYWORDS: sensitized solar cells, CdSe/CdS quantum dots, ZnSe passivation, type II core-shell structure

ABSTRACT

Research on development of efficient passivation materials for high performance and stable quantum dot sensitized solar cells (QDSCs) is highly important. While ZnS is one of the most widely used passivation material in QDSCs, an alternative material based on ZnSe which was deposited on CdS/CdSe/TiO_2 photoanode to form semi core/shell structure has been found more efficient in terms of reducing electron recombination in QDSCs in this work. It has been found that the solar cell efficiency was improved from 1.86% for ZnSe0 (without coating) to 3.99% using 2 layers of ZnSe coating (ZnSe2) deposited by successive ionic layer adsorption and reaction (SILAR) method. The short circuit current density (J_{sc}) increased nearly one fold (from 7.25 mA/cm^2 to13.4 mA/cm^2) and the open circuit voltage (V_{oc}) was enhanced by 100 mV using ZnSe2 passivation layer compared to ZnSe0. Studies on the light harvesting efficiency (η_{LHE}) and the absorbed photon-to-current conversion efficiency (APCE) have revealed that the ZnSe coating layer caused the enhanced η_{LHE} at wavelength beyond 500 nm and a significant increase of the APCE over the spectrum of 400-550 nm. A nearly 100% APCE was obtained with ZnSe2, indicating the excellent charge injection and collection process in the device. The investigation on charge transport and recombination of the device has indicated that the enhanced electron collection efficiency and reduced electron recombination should be responsible for the improved J_{sc} and V_{oc} of the QDSCs. The effective electron lifetime of the device with ZnSe2 was nearly 6 times higher than ZnSe0 while the electron diffusion coefficient was largely unaffected by the coating. Study on the regeneration of QDs after photo-induced excitation has indicated that the hole transport from QDs to the reduced species (S^{2-}) in electrolyte was very efficient even the QDs were coated with a thick ZnSe shell (three layers). For comparison, ZnS coated CdS/CdSe-sensitized solar cell with optimum shell thickness was also fabricated, which generated a lower

energy conversion efficiency (η = 3.43%) than ZnSe-based QDSC counterpart due to a lower V_{oc} and FF. This study suggests that ZnSe may be a more efficient passivation layer than ZnS attributed to the type II energy band alignment of the core (CdS/CdSe quantum dots) and passivation shell (ZnSe) structure, leading to more efficient electron-hole separation and slower electron recombination.

1. Introduction

Quantum dots-sensitized solar cells (QDSC) are devices which adopt a similar device structure with traditional dye-sensitized solar cells (DSSC) but using semiconductor quantum dots (QDs) as light absorbing material. Generally speaking, QDSC consist of QDs coated TiO_2 based mesoporous film as photoanode, a liquid electrolyte containing S^{2-}/S_n^{2-} based redox couple, and a counter electrode. QDs are particles with sizes less than the Bohr radius for that material. Due to quantum confinement, QDs possess unique optical and electronic properties such as particle size-dependent energy band gap and optical properties as well as multiple exciton generation.[1-4] The light absorption coefficient of QDs is normally in the order of 10^5 cm^{-1},[5-6] which is ten times higher than the light absorption of the well-known light absorber based on ruthenium-complex dye. In addition, the dipole property of QDs is also believed to benefit the interfacial charge separation process in QDs solar cells. Because of these merits, it is predicated that the theoretical solar energy conversion efficiency of QDs-based solar cells is around 44%,[7] which is much higher than the Shockley-Queisser energy conversion limit for a single junction solar cell (31-33%).

Materials based on CdS and CdSe are the most widely investigated semiconductor QDs for QDSC owing to their easy synthesis.[3, 8] CdS/CdSe QDs can be deposited on TiO_2 film by a

method called successive ionic layer adsorption and reaction method (SILAR). In this method, a TiO_2 film was dipped in a solution of Cd^{2+} and then in S^{2-}/Se^{2-} containing solution in sequence to complete one deposition cycle for formation of CdS or CdSe. The particle size of the QDs is controlled by the number of deposition cycle. The QDs that are introduced to the TiO_2 film by SILAR directly contact with TiO_2 nanoparticles, which is believed to benefit a more efficient charge transfer of the device.[9]

Although many efforts have been made in the past, the performance of QDSC still significantly lags behind that of DSSC due to a more serious charge recombination process and lower QDs coverage in the photoanode. So far, the best efficiency with DSSC is 13% while the performance of champion QDSC is around 7%.[10-11] Thus, an in-depth understanding of the parameters that govern the performance of QDSC is important for developing new strategies for improving the device performance.

Similar to DSSC, the performance of a QDSC is controlled by the competition between the desirable process of photo-induced electron generation and subsequent electron injection and collection and the process of electron recombination.[12-14] However, compared to DSSC, QDSC suffer a much more complex electron recombination process.[15-16] Besides the charge recombination with oxidized species in liquid electrolyte which is normally the main recombination route in DSSC, the charge recombination process in QDSC also includes the recombination of photogenerated electron with hole of QDs and with oxidized species of the electrolyte before electron injection; and after electron injection, the back reaction of the injected electron at the conduction band of TiO_2 with hole of QDs and with surface defects of TiO_2. These processes are much more serious than those in traditional DSSC. As a consequence, both the electron injection efficiency and electron collection efficiency of QDSCs are generally lower

compared to DSSCs.[7, 15, 17-18] In addition, Zhu *et al* have reported that Auger recombination in QDs due to surface charging by ploysulfide electrolyte can also impede the charge transfer from QDs to TiO_2, resulting in reduced charge injection efficiency.[19]

Besides device performance, stability is another important issue related with QDSCs. Due to their extremely small particle size, QDs normally possess a much higher density of surface defects in the form of dangling bonds. Under illumination, free radicals generated by the dangling bond can interact with species such as oxygen, resulting in oxidization of QDs.[20]

To address above issues, researchers have developed a strategy based on surface coating CdS or CdSe QDs with a passivation shell layer of large bandgap material such as ZnS to protect QDs from photodegradation and to reduce recombination in QDs.[20-22] Compared to CdSe and CdS, ZnS has a more negative minimum conduction band edge (E_{cb}) and a more positive maximum valence band edge (E_{vb}), leading to a Type I energy alignment of the core/shell structure. In this structure, the energy barrier of the ZnS shell prevents the transport of both electron and hole from QDs to electron and hole acceptor species in the liquid electrolyte. As a consequence, although the electron back reaction from QDs to the electrolyte is suppressed, the hindrance of the desired hole transport from QDs to the electrolyte causes reduced charge separation in QDs.[22] Hence, a delicate control of the thickness of the shell passivation layer to ensure that the benefit from the reduced recombination surpasses the loss in charge separation is very critical for improving the performance of QDSCs.

Nevertheless, theoretically the negative impact of the passivation layer on charge separation in QDSC can be overcome using a type II core/shell energy alignment. In Type II core/shell structure, both the E_{cb} and E_{vb} of the shell material are higher than those of the core material.

Hence, the transport of hole from QDs core to the shell material is energetically favorable while the transport of electron from QDs to the shell is blocked. As a consequence, an efficient charge separation and reduced electron recombination can be achieved. Through material screening, we have found that ZnSe is one of such suitable passivation materials for CdSe/CdS QDs to form a type II core-shell structure. The schemes showing the structure of the photoanode of the QDSC and the energy band alignment of the materials involved in the photoanode are illustrated in Figure 1(a, b). As illustrated in Fig. 1 (b), the E_{vb} of ZnSe is higher than that of both CdS and CdSe but is more negative than the redox potential of sulfide/polysulfide, enabling the transfer of hole from CdSe/CdS to ZnSe then to sulfide/polysulfide feasible. Meanwhile, due to the more negative E_{cb} of ZnSe compared to that of CdSe and CdS, the electron transfer from CdS/CdSe QDs to S_n^{2-} in the electrolyte is blocked, forcing the injection of electron to TiO_2. The benefit of ZnSe as a type II shell layer on device performance has been reported with $CuInS_2$ and CdSe based QDSCs.[23] In addition, Yan *et al* have reported accelerated charge separation and more efficient charge collection with solar cells sensitized with ZnSe/CdSe/ZnSe quasi-quantum well.[24] In addition, a strong charge separation in CdS/ZnSe core/shell nanoparticles was also observed by Boldt *et al*.[25] More recently, Soni *et al*., have reported that thicker ZnSe shell in CdSe/CdS/ZnSe "QD/shell" structure did not harm their device performance. Instead it contributed to a better electron-hole pair separation thanks to the Type II energy band alignment.[26] Similar phenomenon has also been reported by Ivanov *et al*.[27] and Verma *et al.* [28] respectively.

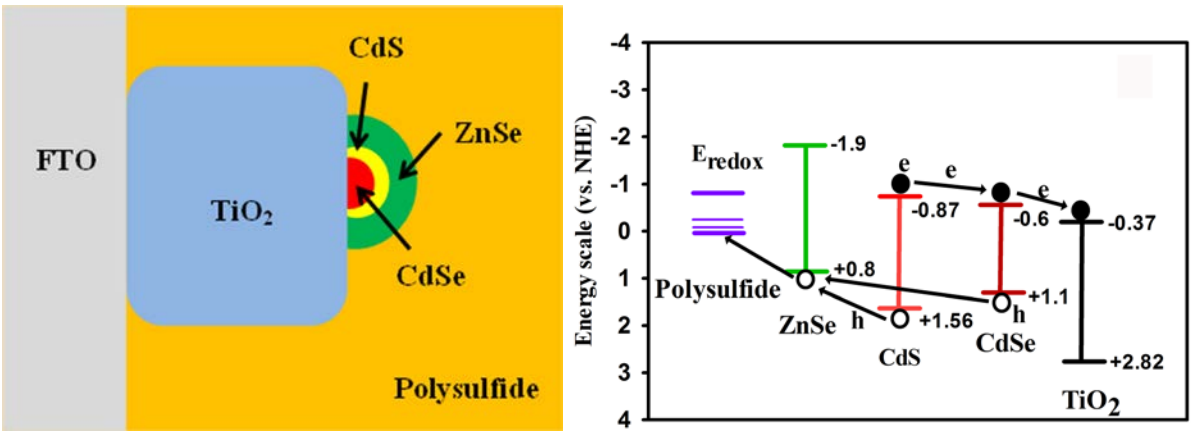

(a) (b)

Figure 1. Schematic diagram of the photoanode (a) and the energy band alignment of the materials for the ZnSe/CdS/CdSe quantum dots solar cell (b).

Despite this, research on QDSC based on CdS/CdSe QDs using ZnSe as shell layer is still very limited, in particular the impact of ZnSe coating on the charge transport and recombination of the device is not well understood. In this work, we have investigated the effect of ZnSe coating layer on the performance and charge transport and recombination of CdS/CdSe -sensitized solar cells. It has been found that, compared to the device without ZnSe shell, a nearly two-fold enhancement of the energy conversion efficiency was achieved with the CdS/CdSe based QDSC with a two SILAR layers of ZnSe coating (ZnSe2). The study on electron transport and recombination has confirmed that the ZnSe coating layer significantly suppressed the electron recombination in the solar cells. In the meantime, the transport of hole from the QDs to the reduced species (S^{2-}) of the liquid electrolyte was still very efficient even with thick ZnSe coating (3 layers), suggesting a high charge separation process.

2. Experimental

Fabrication of CdS/CdSe sensitized TiO_2 film

All the chemicals used in this work were purchased from Sigma Aldrich unless otherwise stated.

A TiO_2 compact layer was deposited on a clean fluorine doped tin-oxide (FTO, TEC15, 2.2 mm thickness, Pilkington) glass substrate by spray pyrolysis according to the procedure reported previously.[29-30] After that, a layer of TiO_2 film was deposited by doctor-blading using a commercial paste (Dyesol DSL, 18NR-T). The films were allowed to relax in air for a couple of minutes and dried on a hotplate at 100°C for 10 minutes before being sintered at 500°C for 30 minutes to remove all organic materials to form a mesoporous structure. The thickness of the film was around 12 μm and the average TiO_2 particle size was around 20 nm.

The procedure for deposition of CdSe and CdS nanocrystals on the TiO_2 film by successive ionic layer adsorption and reaction (SILAR) was reported previously.[8, 31] Briefly, the TiO_2 film was firstly dipped in 0.02 M $Cd(NO_3)_2.4H_2O$ methanol aqueous solution (methanol/water=1:1, v/v) to adsorb a layer of Cd^{2+} on TiO_2 surface. After washing to remove excessive Cd^{2+}, the film was then immersed in a Se^{2-} precursor solution for 1 min to complete one deposition cycle. The Se-precursor solution was prepared by dissolving 0.03 M SeO_2 and 0.06 M $NaBH_4$ in absolute ethanol in a three neck flask under nitrogen atmosphere.[32] The solution was magnetic stirred for around 75 - 90 mins until it became semi-transparent with dark maroon color. The color of the sensitized TiO_2 films changed from white to maroon with the increase of deposition cycle of CdSe. Through optimized deposition procedure, five SILAR deposition cycles of CdSe (CdSe5) were used in this work, which produced CdSe QDs with average particle size around 3.9 nm as determined by HR-TEM based on the measurement of at least 200 particles.[20]

The CdSe-sensitized photoanode was subsequently dipped in 0.02 M $Cd(NO_3)_2.4H_2O$ in methanol and then in 0.02 M $Na_2S.9H_2O$ in methanol/water (1:1, v/v) solution for one minute each to load CdS QDs. The film was rinsed with methanol solvent for 1 minute and then dried by blowing nitrogen gas. 5 SILAR deposition cycles for CdS were adopted to make CdS/CdSe/TiO_2 film. The average particle size of the deposited CdS was around 3.0 nm.[20]

The ZnSe coating layer was deposited on the CdS/CdSe/TiO_2 film via SILAR method as well. Briefly, 0.1 M Se-precursor solution was prepared by mixing 0.1 M SeO_2 and 0.2 M $NaBH_4$ in deionised water in a three-neck flask. The solution was magnetic stirred for one hour until it became transparent. The CdS/CdSe-sensitized TiO_2 electrode was dipped in 0.1 M $Zn(CH_3COO)_2.2H_2O$ aqueous solution and then in the prepared Se-precursor solution to complete one deposition layer of ZnSe (ZnSe1). The same procedure was repeated when depositing a thicker ZnSe shell. For clarity, the different SILAR coating layer, N, is shown by ZnSeN (N = 0 - 3) in the following. The prepared ZnSe/CdS/CdSe/TiO_2 photoanode was stored in a petri dish covered with Al foil to prevent possible photodegradation before cell assembly. It is worth to mention that the attempt to see the difference in the SEM images of the TiO_2 film coated with or without CdSe/CdS/ZnSe quantum dots was failed due to the extremely thin layer of QDs particles.

The ZnS coating layer with optimum thickness (2 SILAR deposition layers, ZnS2)) was prepared using 0.1 M $Zn(CH_3COO)_2.2H_2O$ and 0.1 M $Na_2S.9H_2O$ aqueous solution as the precursor solution for Zn^{2+} and S^{2-} respectively. One minute of dipping in each precursor solution and then rinsing in deionised water were performed for ZnS deposition.

Fabrication of quantum dot sensitized solar cells

Cu_2S counter electrode for the QDSCs was made using a brass foil (Cu:Zn = 64:27) which was firstly treated in 32% HCl solution at 70°C for 20 minutes to dissolve Zn. The foil was then dried on a hotplate at 100°C for one hour before being dipped in a polysulfide electrolyte solution consisting of 1 M sulfur, 1 M $Na_2S.9H_2O$ and 0.1 M NaOH in methanol/water (7:3 v/v) for 20 minutes to form Cu_2S. The electrode was then dried on a hotplate before being used to assemble solar cells. QDSC was assembled by sealing the prepared QDs-sensitized photoanode with the Cu_2S counter electrode together using a Surlyn film (Solarnix, 25 μm) as spacer. The distance between the electrodes was filled with a polysulfide liquid electrolyte with the same compositions as used to make Cu_2S electrode.

Material and device characterization

The light absorbance and transmittance of the CdS/CdSe co-sensitized TiO_2 films with different ZnSe coating layer was determined by a UV-visible spectrophotometer (Varian Cary 50) and the reflectance of the photoanode was measured by a UV-visible spectrometer with integrated sphere (Varian, Cary 5000). The current density (J) - voltage (V) performance of the CdSe/CdS-sensitized solar cells was measured with a solar simulator equipped with 150 W Xenon lamp. A reference silicon solar cell (Fraunhofer ISE) was employed to calibrate the illumination intensity of the solar simulator to 100 mW/cm^2 (AM1.5). At least three cells were made for each ZnSe coating layer. The incident photon-to-current conversion efficiency (IPCE) spectra of the QDSC was measured as a function of wavelength provided by a 150 W Xe lamp light source coupled to a monochromater (Cornerstone 260). The photocurrent generated by the cell at each wavelength was recorded by a source measurement unit (Keithley 236). The photovoltage decay of the cell was recorded using an electrochemical workstation (VersaSTAT3) after switching off the light source which was provided by a light emitting diode (LED, 627 nm).[14]

The stepped light-induced measurement of photocurrent and photovoltage (SLIM-PCV) was used to determine the effective electron lifetime (τ_n) and electron diffusion coefficient (D_n) of the solar cell.[33] The measurement was performed using a freshly prepared device and using a 635 nm diode laser as the light source. The J_{sc} or V_{oc} decays were obtained at different laser intensity recorded by a multimeter (ADCMT 7461A). For electron lifetime measurement, the laser intensity was stepped down to provide a small voltage change (less than 1 mV). For D_n measurement, the laser intensity was stepped down to obtain less than 10% change in the photocurrent. The electron density (n_t) in the photoanode film was determined by charge extraction method using a nanosecond switch (AsamaLab).[34] To enhance the signal of the measurement, the photoanode with thickness of TiO_2 film around 7.0 μm was used in the SLIM-PCV measurement.

Transient absorption spectroscopy (TAS) was used to monitor the lifetime of photogenerated species of the QDs-sensitized photoanode on the nanosecond to millisecond timescale. The CdS/CdSe QDs-sensitized TiO_2 film was covered by a slice of FTO glass (2.2 mm, 7 Ω/square, TEC®) coated with a thin layer of platinum and sandwiched with a Surlyn film (25 μm) acting as a spacer. The space between the photoanode and the Pt coated FTO electrode was filled with S^{2-}/S_n^{2-} redox electrolyte with the same composition to the one used for QDSC. An inert electrolyte composed of 1M NaOH in methanol/water (7:3, v/v) was used to measure the charge recombination in QDs in the absence of electron and hole acceptor in the electrolyte. Six to eight nanosecond pulse width laser pulses using a Q-switched Nd-YAG laser (532 nm, 10 Hz, INDI Quanta-Ray, Spectra-Physics) were used to photoexcite the QD-sensitized TiO_2 film (pump). The probe wavelength was 700 nm and was provided by a current-controlled (BENTHAM 605) quartz halogen lamp (IL1). A 700 nm band pass filter was employed between the probe lamp and

the sample to prevent photoexcitation of the sample by the probe beam. A system consisting of monochromator (CM110, SP), a silicon photoreceiver (HCA-S-200M, Germany) and a digital oscilloscope (DPO 4054, Tektronix) was used to record the optical signals. A previous study by Palomares *et al*. has assigned the transient absorption signal at 700 nm to photoinduced holes in the CdS/CdSe QDs following electron injection into TiO_2.[18] Similar consideration was also used in this work. The TA signals were averaged using 512 laser pulses at 1 Hz by picking only one pulse per every ten using a laser shutter controlled by a digital delay generator (DG535, Stanford Research). The time resolution of the setup was around 100 ns.

Results and Discussion

Solar cell performance

The performance of the solar cells with different ZnSe shell layer on CdS/CdSe/TiO_2 film is shown in Figure 2. One striking feature that can be seen in Figure 2(a) is that, compared to the cell without coating (ZnSe0), the photocurrent density of the cell with ZnSe coating is much higher, a phenomenon normally observed in QDSC using passivation layer.[21, 35-36] The short-circuit current density (J_{sc}) of the solar cell increases with the increase of the coating layer up to 2 (ZnSe2). The J_{sc} increases significantly from 7.25 mA/cm^2 for ZnSe0 to 10.6 mA/cm^2 for ZnSe1. And a further increase of J_{sc} is obtained with ZnSe2 with J_{sc} = 13.4 mA/cm^2. In the meantime, the V_{oc} of the cell is enhanced with ZnSe coating until ZnSe2 which produced a 100 mV higher V_{oc} compared to that of ZnSe0. As a consequence, the conversion efficiency of the solar cell is increased over one fold from 1.86% for ZnSe0 to 3.99% for ZnSe2. Nevertheless, further increase of the thickness of shell layer to ZnSe3 leads to the decrease of both the J_{sc} and

V_{oc} of the solar cell. The characteristic parameters for the performance of the solar cells are summarized in Table 1.

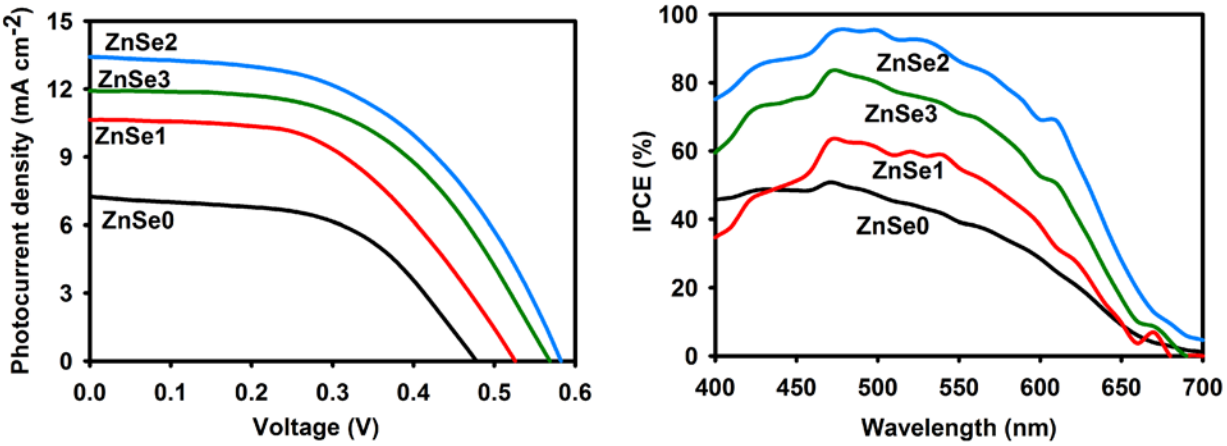

(a) **(b)**

Figure 2. *J-V* (a) and IPCE (b) plots for the CdS/CdSe-sensitized solar cells with different ZnSe coating layer.

Table 1. Characteristic parameters for the performance of the CdSe/CdS-sensitized solar cells with different ZnSe coating layer.

ZnSe layer	***η* (%)**	**V_{oc} (mV)**	**J_{sc} (mA/cm^2)**	***FF***
0	1.86	489	7.25	0.52
1	2.82	538	10.6	0.49
2	3.99	580	13.4	0.51
3	3.56	567	11.9	0.53

The plots of incident photon-to-current conversion efficiency (IPCE) of the corresponding cells are shown in Figure 2(b). It is known that J_{sc} of a solar cell is the integration of IPCE over the solar spectrum of interest. As expected, the IPCE shows the trend of ZnSe0 < ZnSe1 < ZnSe3 < ZnSe2, which is consistent with the variation of J_{sc} of corresponding cells. It is noticed that the QDSC with ZnSe coating show much higher IPCE in the spectral wavelength range from 400 to 600 nm. Especially, the IPCE for ZnSe2 is over 80% in the spectral wavelength range of 420-600 nm, indicating the excellent energy conversion efficiency. Nevertheless, the IPCE drops significantly at the wavelength beyond 600 nm for all the devices, which is mainly due to the decreased light absorption as indicated by the light absorption spectrum of the corresponding photoanode for these devices in Fig. 3(a). The light absorption spectrum of the CdS/CdSe/TiO_2 photoanode with different ZnSe coating layer (Figure 3(a)) reveals that the light absorption of all the photoanode with ZnSe coating is close to unity at the spectral wavelength below 550 nm. For the film without ZnSe coating, a nearly 100% light absorption is obtained in the wavelength range between 400-500 nm. The light absorption of the photoanodes decreases at the wavelength beyond 550 nm. However, the extent of the decrease is different, leading to higher light absorption obtained with the photoanode with thicker ZnSe coating compared to the film with thinner shell layer.

$$IPCE = \eta_{LHE} \times \eta_{inj} \times \eta_{coll} = \eta_{LHE} \times APCE \qquad \text{(Eq1)}$$

IPCE of a QDSC depends on three parameters according to Eq1: 1) light harvesting efficiency (η_{LHE}); 2) electron injection efficiency (η_{inj}); and 3) electron collection efficiency (η_{coll}). In order to find out which parameter(s) is responsible for the change of J_{sc}, the η_{LHE} of the device with different ZnSe coating layer was determined by measuring the light absorption coefficient (α)

and the thickness (d) of the sensitized TiO_2 film (LHE = 1-exp(-αd)) according to the method reported previously .[37-38] The light absorption coefficient was determined by $\alpha = -\frac{1}{d}\ln(\frac{T_{QD/TiO2}}{T_{TiO2}})$ where $T_{QD/TiO2}$ is the transmittance of the QDs coated photoanode and T_{TiO2} is the transmittance of bare TiO_2 film. The light reflectance due to scattering of QDs nanoparticle is assumed weak and is not considered here. The η_{LHE} of the photoanode with different ZnSe coating layer is shown in Figure 3(b). Apparently, the trend of η_{LHE} is consistent with the variation of the light absorption of the photoanode with different ZnSe coating layer. However, as mentioned above, the light scattering of QDs particles was not considered in the calculation of η_{LHE}. Nevertheless, as shown in Figure 3(c), all the photoanodes show significant light reflectance at spectral wavelength beyond 550 nm. Because of this, the calculated η_{LHE} may not be reliable in the longer spectral wavelength over 550 nm. Therefore, the following discussion on the η_{LHE} and APCE of the cells is only focus on the results in the spectral wavelength range of 400-550 nm where the light reflectance is weak and negligible although the results in the whole wavelength (400-700 nm) are shown.

As can be seen in Figure 3(b), the η_{LHE} of all the CdSe/CdS QDs coated TiO_2 film is close to 100% at the spectral wavelength below 500 nm regardless whether a ZnSe coating was used or not, consistent with the strong light absorption of the CdS/CdSe QDs. The result also suggests that the contribution of ZnSe shell to the light absorption of the photoanode is very small at shorter wavelength. In contrast, the contribution of ZnSe passivation layer to the light absorption and the η_{LHE} of the photoanode is clearly seen at the wavelength beyond 500 nm. The η_{LHE} increases with the increase of the coating layer. Theoretically, the energy bandgap of bulk ZnSe is around 2.7 eV, which is very unlikely to contribute the light absorption of the CdS/CdSe/TiO_2

photoanode at wavelength longer than 460 nm. Therefore, the enhanced light absorption at longer wavelength is probably due to the interaction between ZnSe shell and CdS/CdSe QDs because of partial overlap of the exciton wave function of the core (CdSe/CdS) and shell (ZnSe) materials.[39] Similar phenomenon for improved IPCE was also observed in ZnS coated CdSe QDs solar cells.[40]

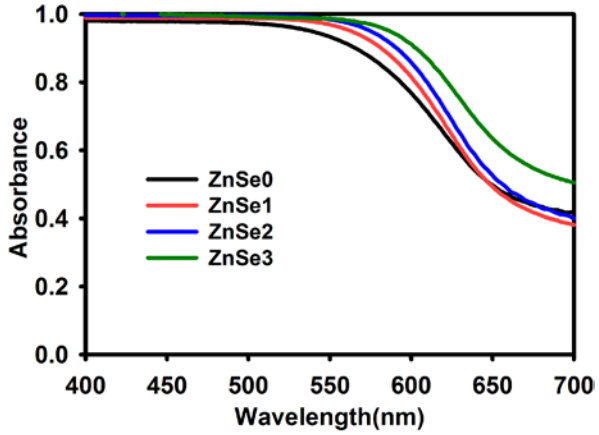

(a)

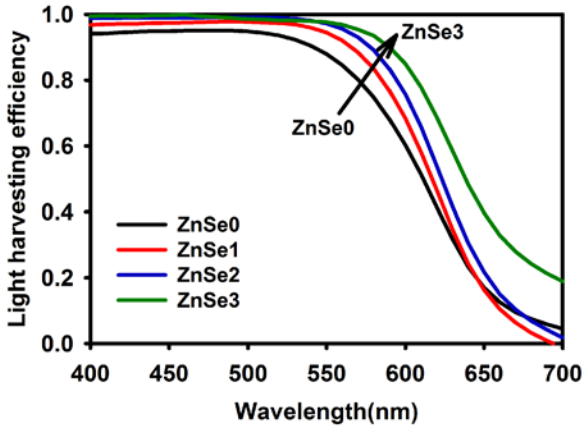

(b)

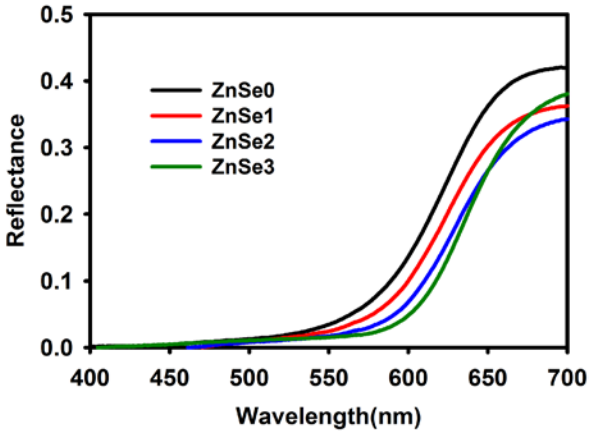

(c)

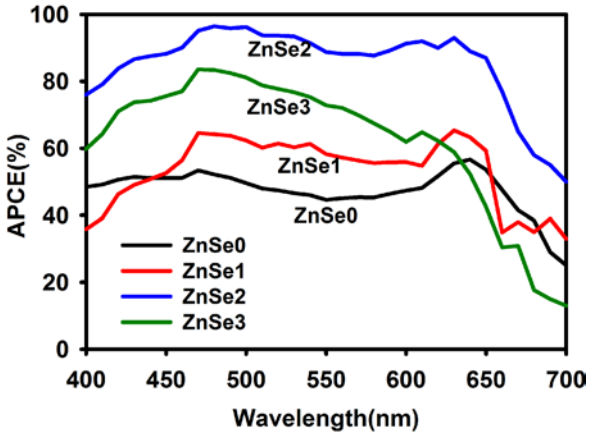

(d)

Figure 3. Comparison of the light absorbance (a); light harvesting efficiency (η_{LHE}) (b); light reflectance (c) and the absorbed photon-to-current conversion efficiency (APCE) (d) for the CdS/CdSe-sensitized solar cells with different ZnSe coating layer.

The absorbed photon-to-current conversion efficiency (APCE) which is the product of η_{inj} and η_{coll} according to Eq1 is shown in Figure 3(d). As can be seen, the APCE of the cells varies in the same trend with IPCE in the wavelength range of 400 nm- 550 nm with ZnSe2 > ZnSe3 > ZnSe1> ZnSe0, which suggests that the change in the light harvesting efficiency of the cell with different ZnSe coating may not be the main reason for the different J_{sc}. Instead, the electron injection efficiency, η_{inj}, and/or electron collection, η_{coll}, should be responsible for the enhanced IPCE and J_{sc}.

η_{inj} of the QDSC is driven by the energy offset (E_{offset}) between the E_{cb} of CdS and CdSe quantum dots and the E_{cb} of bulk TiO_2. As illustrated in Figure 1(b), the theoretical E_{cb} of bulk CdSe and CdS is over 200 mV higher that of TiO_2 and this value should be even higher due to quantum confinement of CdS and CdSe QDs, which leads to upshift of the E_{cb} of the materials. Hence, the E_{offset} should be sufficient to drive the transfer of electron from CdS and CdSe to TiO_2.[41]

Nevertheless, previous research on DSSC has reported that the conduction band of TiO_2 film can be modified by adsorption of material such as ruthenium dye complex because of the acidic nature of the molecule.[14] Such a change in E_{cb} of TiO_2 can in turn cause the variation of E_{offset} and the V_{oc} of the device. Although the surface of TiO_2 is mainly covered with CdSe/CdS QDs and ZnSe is expected to coat on CdS instead of TiO_2 in this work, it cannot rule out that part of TiO_2 surface could be covered by ZnSe nanocrystals, modifying its surface property. Thus it is

necessary to identify the variation of E_{cb} of the photoanode and its effect on the E_{offset} and V_{oc} of the device due to ZnSe coating. The variation of E_{cb} can be determined by monitoring the open circuit voltage of the cell against total electron density.[29] As shown in Figure 4(a), except ZnSe1 which shows a bit higher V_{oc} than the other cell at a constant electron density, the difference in voltage between ZnSe0, ZnSe2 and ZnSe3 is less than 20 mV. Therefore, the influence of ZnSe coating on the conduction band of the CdS/CdSe/TiO_2 film is indeed very small and should not significantly affect the energy driving force for the electron injection from CdSe/CdS QDs to TiO_2 and the V_{oc} of the device.

The efficient electron injection process of the CdS/CdSe solar cells with ZnSe coating is reflected by the very high APCE for the device with ZnSe2. The APCE is over 90% at the wavelength beyond 450 nm. It suggests that the electron injection efficiency of the cell was probably close to 100% and is not the limiting factor for the device performance. However, for other cells, especially the cell without ZnSe coating, the η_{inj} might not be as efficient as the one with coating due to possible electron recombination with polysulfide electrolyte.

The electron collection efficiency in a mesoporous TiO_2 film is governed by the competition between electron transport and electron recombination. It has been well accepted that the transport of electron in a mesoporous TiO_2 film is governed by a process of electron trapping/detrapping.[7, 13, 17, 42-43] In this process, the free electron at the conduction band of TiO_2 falls in the trap states (defects) and then jump back to the conduction band of TiO_2 again if the electron has sufficient energy. The electron which falls in the deep trap states and fails to return to the conduction band of TiO_2 contributes to charge recombination. Due to the trapping/detrapping process, both the effective electron lifetime, τ_n, and the effective electron diffusion coefficient, D_n, in QDSC differ from the electron lifetime and diffusion coefficient of

single crystal TiO_2.[44] The electron diffusion length, L_n, which is the product of D_n and τ_n ($L_n = \sqrt{D_n \tau_n}$), relative to the thickness of TiO_2 film determines the electron collection efficiency.

As shown in Figure 4(b), the D_n of the cell with different ZnSe coating layer are nearly identical, suggesting that the impact of ZnSe coating on D_n is very small. This is just what is expected because the ZnSe nanocrystals mainly anchored on CdS/CdSe QDs rather than on TiO_2 particle. Therefore, it should not affect the surface property of TiO_2 film.

In contrast to D_n, the influence of ZnSe coating layer on τ_n is more pronounced. As shown in Figure 4(c), compared to the cell without coating (ZnSe0), the cell with ZnSe coating show a much higher τ_n. A nearly 6-fold enhancement of τ_n is obtained with ZnSe2. The improved τ_n should be attributed to the suppression of charge recombination between photogenerated electrons from CdSe and CdS QDs with the oxidized species S_n^{2-} in the electrolyte owing to the surface passivation by ZnSe shell and energy barrier provided by the shell.[45] However, τ_n decreases slightly beyond two ZnSe coating layers. The study on the regeneration of cations of QDs with ZnSe3 by transient absorption spectroscopy has confirmed that hole transport in the device was not a problem (Figure 7), ruling out the possibility that the decreased electron lifetime is due to electron recombination in QDs. Hence, the reduced electron lifetime of the cell with ZnSe3 should be related with the increased electron recombination with the electrolyte due to a high density of hole at the ZnSe shell layer. Since the charge separation of type II core-shell alignment increases with the increase of shell thickness,[26-27] it is reasonable to believe that the density of hole in the shell material and density of electron in the core and then in TiO_2 film increase with the shell thickness. The high density of hole in the shell can attract more negatively charged species in the liquid electrolyte including both S^{2-} and S_n^{2-} in the TiO_2 film through static

Coulomb attraction force, resulting in increased charge recombination between free electron on TiO_2 nanoparticles with S_n^{2-}.[46]

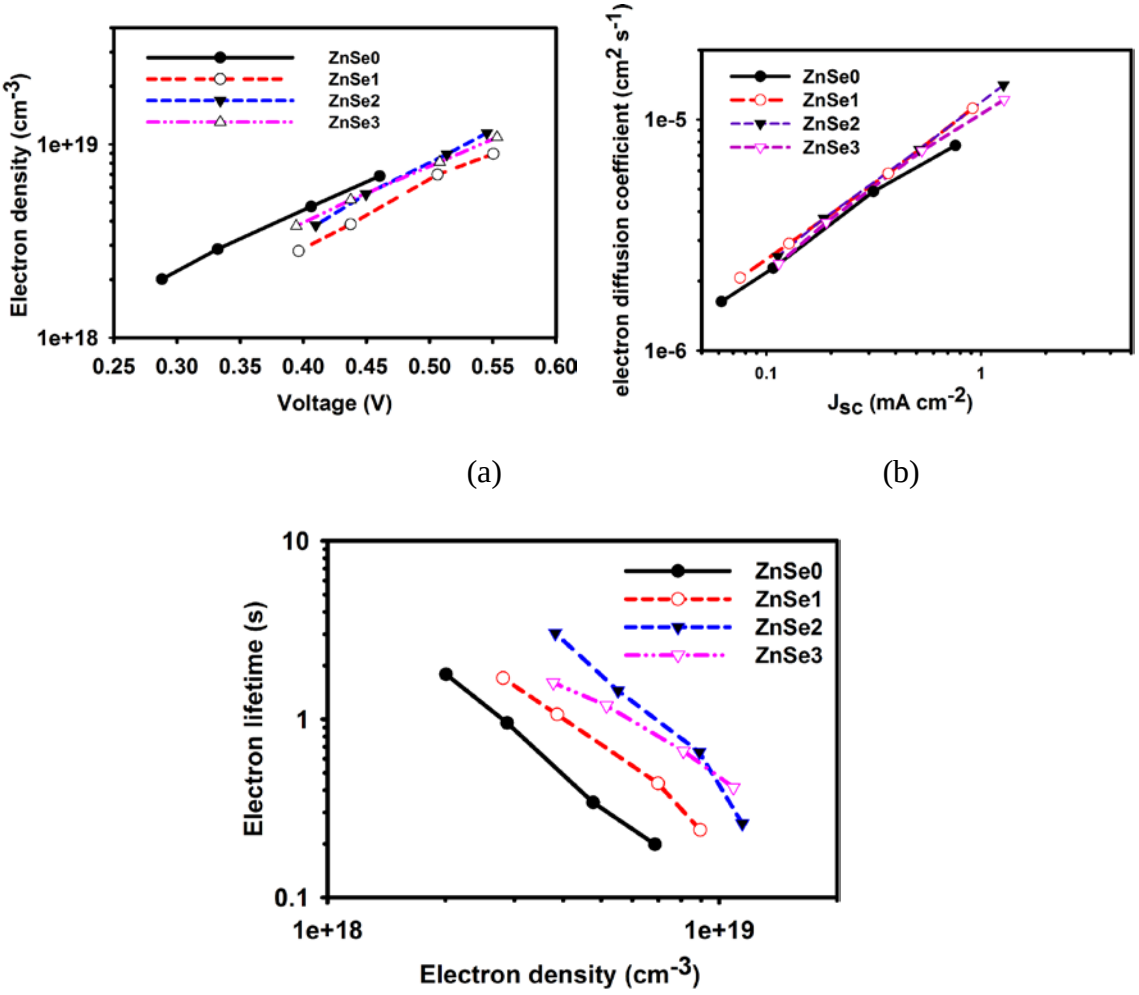

Figure 4. Comparison of the plots of (a) total electron density *vs* voltage; (b) effective diffusion coefficient and (c) effective electron lifetime of the CdS/CdSe sensitized solar cells with different layers of ZnSe shell coating.

Given that D_n is largely unaffected while τ_n is significantly enhanced using ZnSe coating, it is expected that the electron diffusion length, L_n, which is the square root of product of D_n and τ_n

should follow the same trend with τ_n, that is, ZnSe0 < ZnSe1< ZnSe3 < ZnSe2. This is in consistent with the change of J_{sc} and APCE of the cells, explaining that the increase of APCE and J_{sc} should be attributed to the enhanced charge collection efficiency.

Since the ZnSe coating has negligible influence on the E_{cb} of CdS/CdSe sensitized TiO_2 film as shown above, hence we can also investigate the evolution of τ_n by photovoltage decay. As illustrated in Figure 5(a), a very rapid photovoltage decay is observed with ZnSe0. The V_{oc} of the cell decays to nearly zero volt within 10 s in dark. In contrast, the decay is dramatically slowed down with ZnSe coating. The thicker is the coating layer, the slower the photovoltage decays. For the cell with ZnSe3, a voltage of more than 50 mV is still noticeable even after 100s in dark, confirming the charge retention effect of the passivation layer in the photoanode through hindering electron recombination with S_n^{2-} in the electrolyte. The τ_n for the devices with different photovoltage decay behavior was then calculated according to Eq. 2[47] where k_B and q are Boltzmann constant and elemental charge, respectively.

$$\tau_n = -\frac{k_B T}{q}\left(\frac{dV_{oc}}{dt}\right)^{-1} \qquad \text{(Eq.2)}$$

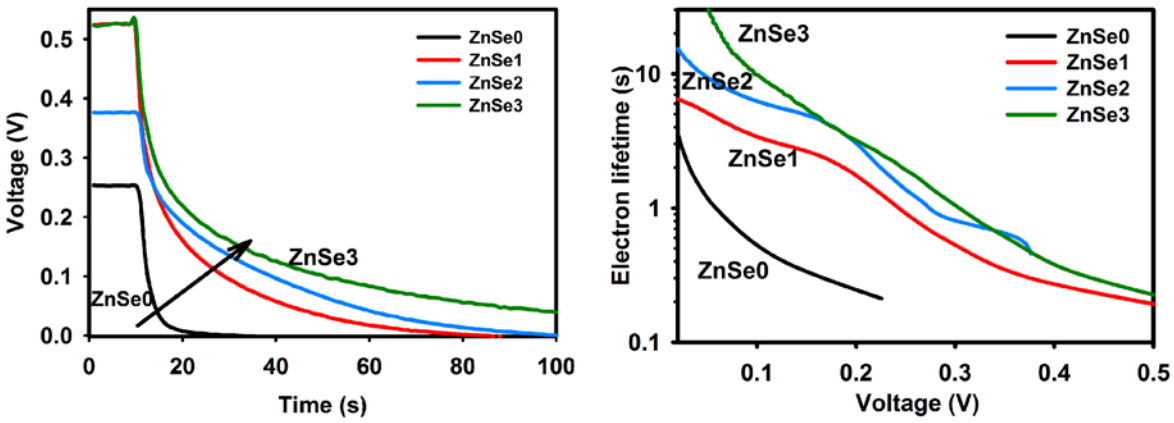

(a) **(b)**

Figure 5. Comparison of the plots of (a) photovoltage decay and (b) the effective electron lifetime of the CdS/CdSe-sensitized solar cells with different ZnSe coating layer.

As illustrated in Figure 5(b), the τ_n of the solar cell increases with the increase of ZnSe coating layer from ZnSe0 to ZnSe2, a trend consistent with the results in Figure 4(c). Nevertheless, the highest τ_n was obtained with ZnSe3 instead of ZnSe2 as shown in Figure 4(c). This discrepancy is ascribed to the approach used to derive the electron lifetime from photovoltage decay. According to Barnes *et al*, the ideality factor of the solar cell should be taken into account when deriving electron lifetime from photovoltge decay plot using Eq 2.[48] However, such factor was not considered in this work. In addition, the different thickness of the TiO_2 films used for the measurement by SLIM-PCV and by photovoltage decay may be another reason for the different results. The thickness of the TiO_2 film for SLIM-PCV measurement in Figure 4 was 7 μm in order to obtain better signals while 12 μm TiO_2 film was used in the device for photovoltage decay measurement.

The enhanced τ_n not only affects J_{sc} through improving the charge collection efficiency but also the open circuit voltage of the solar cell according to Eq. 3.[49]

$$V_{oc} = \frac{kT}{q} In(\frac{I_{inj}}{n_{cb} k_{rb} [S_n^{2-}]}) \qquad \text{(Eq. 3)}$$

Where I_{inj} is the flux of charge injected to TiO_2 film from the light absorber, k is the Boltzmann constant, and T is the absolute temperature, q is the elemental charge; n_{cb} is density of electrons in the conduction band, k_{rb} is the recombination reaction rate with the oxidized species in the electrolyte, which is inverse to τ_n.

In the work, given that the parameters including T and [S_n^{2-}] are constant, the different V_{oc} of the cell is determined by I_{inj}, n_{cb} and k_{rb}. Theoretically I_{inj} is proportional to J_{sc}.[50] In order to determine the effect of I_{inj} on V_{oc} of the cells, the dependence of open circuit voltage on J_{sc} of the cells is compared using a 635 nm LED as light source as shown in Figure 6. It is found that the V_{oc} of the cells at a constant J_{sc} increases with the increase of the ZnSe coating layer. Furthermore, the difference in V_{oc} at a constant J_{sc} is very close to the change of V_{oc} in the *J-V* plot of the devices shown in Figure 2(a). For example, the voltage of ZnSe0 cell is 70 mV lower than that of ZnSe2 in Figure 6, close to the V_{oc} difference of these cells (91 mV) in Figure 2. It suggests that I_{inj} is not the main reason for the different V_{oc}. In addition, as shown in Figure 4 (a), the conduction band of the cells is very similar (difference is less than 50 mV) and Figure 4(c) shows the trend of electron lifetime at a constant electron density is similar to the change of V_{oc} of the cells. It infers that the enhanced V_{oc} of the cell with ZnSe coating should be mainly attributed to the enhanced τ_n (reduced k_{rb}).

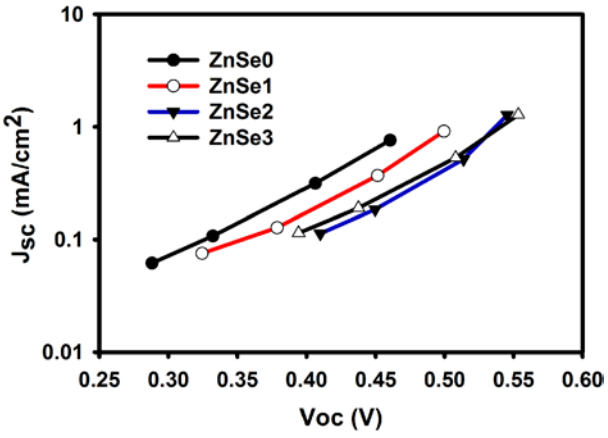

Figure 6. Comparison of plots of J_{sc} vs open circuit voltage of the CdS/CdSe-sensitized solar cells with different ZnSe coating layer

Electron – hole recombination and hole regeneration dynamics using transient absorption spectroscopy (TAS)

It is usually believed that a shell layer may impede the transport of hole from QDs to the reduced species in the electrolyte because of the increased spatial distance. To test whether the hole transport in the QDSC device is efficient or not and whether it is a performance limiting factor, the recombination and regeneration of photon-induced holes in the CdS/CdSe with TiO_2 electrons or with polysulfide electrolyte was studied using the cell with the thickest ZnSe coating (ZnSe3) by transient absorption spectroscopy (TAS). The absorption of the photoinduced holes of CdS/CdSe in the TAS at 700 nm probe wavelength overlaps with the weak absorption by trapped TiO_2 electrons.[18] The transient absorption traces measured for a ZnSe3 sample in an inert electrolyte (black) and in the same electrolyte but containing the polysulfide mediator (red) are shown in Figure 7. The TAS spectra were fitted according to a stretched exponential function as shown in Eq. 4 to 6. The detailed fitting parameters for both hole and electron are shown in Table 2. [51]

$$\Delta OD(t) = \Delta OD_{t=0}(h^+)e^{-(\frac{t}{\tau_{WW}(h^+)})^{\beta(h^+)}} + \Delta OD_{t=0}(e^-)e^{-(\frac{t}{\tau_{WW}(e^-)})\beta(e^-)} \quad (4)$$

$$\tau_{obs} = \frac{\tau_{WW}}{\beta}\Gamma(\frac{1}{\beta}) \quad (5)$$

$$\Gamma\left(\frac{1}{\beta}\right) = \int_0^\infty u^{\frac{1}{\beta}-1}e^{-u}du \quad (6)$$

where ΔOD (t) is the change of optical density with time (t); $\Delta OD_{t=0}$ is the initial change in absorption magnitude for holes (h^+) or for TiO_2 (e^-); β is the stretching parameter; τ_{WW} is the

characteristic stretched relaxation time; Γ() is the gamma function; and τ_{obs} is the observed lifetime representing the mean of the distribution of lifetimes.

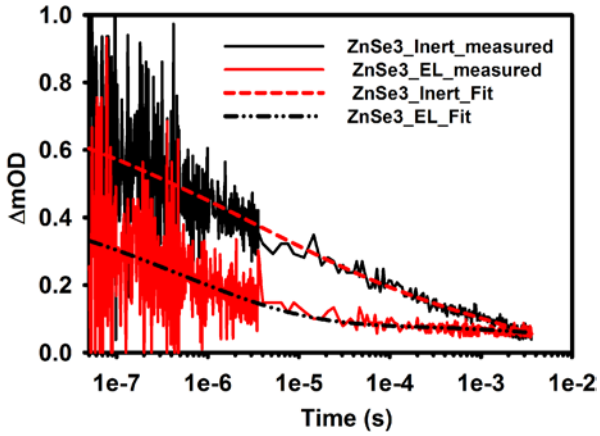

Figure 7. Transient absorption spectra and corresponding fitting curves of ZnSe3 coated CdS/CdSe/TiO_2 photoanode in the absence (denote as inert) and presence of S^{2-}/S_n^{2-} redox couple in the electrolyte (denote as EL).

As shown in Table 2, the observed hole lifetime, $\tau_{obs}\_h^+$, is two orders of magnitude longer in the absence than that in the presence of the polysulfide electrolyte with $\tau_{obs}\_h^+ = 4.33\times10^{-4}$ s for inert electrolyte and $\tau_{obs}\_h^+ = 4.07\times10^{-6}$ s for polysulfide electrolyte, respectively. It indicates highly efficient regeneration efficiency of the ZnSe3/CdS/CdSe QDs even with the thick shell coating. The cell with thinner ZnSe shell should be more efficient due to the reduced spatial distance for charge transfer between CdS/CdSe QDs and the sulfide/polysulfide electrolyte. The photogenerated electron in the photoanode recombines with hole of QDs when the photoanode contacts with the inert electrolyte. In contrast, in the presence of the polysulfide electrolyte, electron transfer of S^{2-} in the electrolyte to the valence band of ZnSe/CdS/CdSe core-shell QD intercepts the recombination of hole with TiO_2 electrons, leading to an initial faster decay of the TA signal. As a result, the lifetime of CB electrons in the TiO_2 in the presence of polysulfides

electrolyte increase, which is reflected as the long but weak TA signal extending into the millisecond timescale. These results are qualitatively similar to that reported by Palomares et al.,[18] suggesting that regeneration of QDs is not the limiting factor for the performance of QDSC with ZnSe coating. It is worth to note that TAS measurement of un-coated Cd/CdSe-sensitized TiO_2 photoanode were also attempted, but the results were inconclusive possibly due to photo-degradation of the uncoated photoanode especially in the inert electrolyte.[20]

Table 2. Summary of the fitting parameters for the transient absorption spectrum of both hole and electron in TiO2 using ZnSe3 coated CdS/CdSe/TiO_2 photoanode.

Fitting parameters for hole:

Electrolyte	$\Delta OD\_h^+{}_{t=0}$	$\tau_{ww}\_h^+$ (s)	β_h^+	Γ_h^+	$\tau_{obs}\_h^+$ (s)
Inert	8.00E-04	3.61E-06	0.20	24.00	4.33E-04
redox electrolyte	4.04E-04	5.23E-07	0.31	2.41	4.07E-06

Fitting parameters for TiO_2 electron (e^-):

Electrolyte	$\Delta OD\_e^-{}_{t=0}$	$\tau_{ww}\_e^-$ (s)	β_e^-	Γ_e^-	$\tau_{obs}\_e^-$ (s)
Inert	8.11E-05	5.29E-03	0.89	0.94	0.006
redox electrolyte	8.11E-05	3.39E-02	0.50	1.00	0.07

Comparison of ZnSe with ZnS passivation coating

The CdS/CdSe QDSC with optimum ZnS coating layer (two SILAR layers) was also prepared to compare with the device with ZnSe2 passivation coating. The comparison of the *J-V* plots of the cells is shown in Figure 8(a). Interestingly, the same J_{sc} (13.4 mA/cm^2) was generated by both cells. However, compared to the cell with ZnSe2 coating, the device with ZnS coating has a

slightly lower V_{oc} and *FF*, leading to lower performance (3.43%). The investigation on the electron recombination of the devices by photovoltage decay shows that ZnSe2 based cell has a slightly higher τ_n than ZnS2 (Figure 8(b)), which is also demonstrated by the slower decay plot of ZnSe2 compared to ZnS (inset in Figure 8(b)). This may explain the slightly higher V_{oc} of the former. This result suggests that the ZnSe may be a more efficient passivation material than ZnS for suppression of electron recombination and facilitation of charge separation in QDSCs.

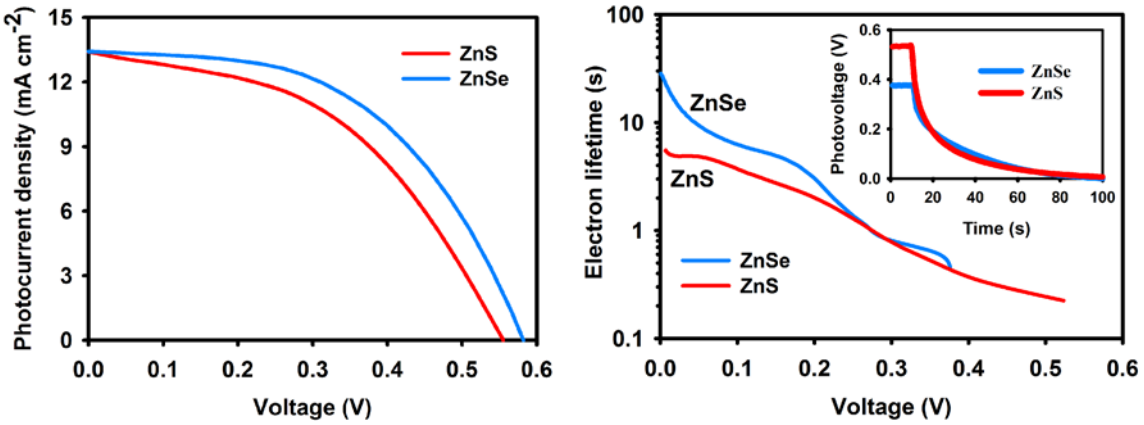

(a) **(b)**

Figure 8. Comparison of the plot of (a) J-V and (b) electron lifetime as a function of voltage for CdSe/CdS-sensitized solar cells with ZnSe and ZnS coatings (two layers). Inset: photovoltage decay plots of the devices.

Conclusions

This work has demonstrated clearly that the performance of CdSe/CdS QDs -sensitized solar cell could be significantly improved using ZnSe shell layer. The efficiency of the solar cells increased from 1.86% (with no coatings) to 3.99% using ZnSe2 shell layer (ZnSe2) owing to the significantly improved V_{oc} and J_{sc}.

The investigation of the charge transport in the photoanode by transient photovoltage decay and photocurrent spectroscopy has confirmed that the effective electron lifetime was improved up to 6 times with two layer of ZnSe coating compared to the cell without coating. In the meantime, it is found that the impact of the passivation layer on the electron diffusion coefficient of the solar cell was very small. As a consequence, the electron diffusion length of the device is expected to vary in the sequence of ZnSe2 > ZnSe3 > ZnSe1 > ZnSe0, consistent with the J_{sc} and IPCE. Therefore, it is believed that the enhanced electron diffusion length with ZnSe shell should be responsible for the enhanced J_{sc} of the QDSC through increasing the charge collection efficiency of the device. However, further increase the thickness of the shell to ZnSe3 led to the reduced electron lifetime although the hole transport from QDs to polysulfide electrolyte of the ZnSe3 device was still very efficient. This suggests that thickness of the shell layer for type II alignment still needs to be carefully controlled for optimum device performance. In addition, comparing to the QDSCs using ZnS coating, the cell with ZnSe coating produced a better performance because of a lower electron recombination. It suggests that ZnSe may be a more efficient passivation material for QDSCs.

Acknowledgements

H.W thanks Australian Research Council (ARC) Future fellowship scheme (FT120100674) for the financial support for this work. A.R thanks the scholarship for PhD *via* Vice-Chancellor Research Fellowship scheme of Queensland University of Technology. The authors thank Mr. Teng Wang for the assistance in measuring the UV-Visible spectra shown in this work.

References

1. Nozik, A. J.; Beard, M. C.; Luther, J. M.; Law, M.; Ellingson, R. J.; Johnson, J. C. Semiconductor Quantum Dots and Quantum Dot Arrays and Applications of Multiple Exciton Generation to Third-Generation Photovoltaic Solar Cells. *Chem. Rev.* **2010**, *110*, 6873-6890.
2. Ruhle, S.; Shalom, M.; Zaban, A. Quantum-Dot-Sensitized Solar Cells. *Chemphyschem* **2010**, *11*, 2290-2304.
3. Kamat, P. V. Quantum Dot Solar Cells: The Next Big Thing in Photovoltaics. *J. Phys. Chem. Lett.* **2013**, *4*, 908-918.
4. Peter, L. M. The Gratzel Cell: Where Next? *J. Phys. Chem. Lett.* **2011**, *2*, 1861-1867.
5. Jasieniak, J.; Smith, L.; van Embden, J.; Mulvaney, P.; Califano, M. Re-Examination of the Size-Dependent Absorption Properties of Cdse Quantum Dots. *J. Phys.Chem. C* **2009**, *113*, 19468-19474.
6. Yu, W. W.; Qu, L. H.; Guo, W. Z.; Peng, X. G. Experimental Determination of the Extinction Coefficient of Cdte, Cdse, and Cds Nanocrystals. *Chem. Mater.* **2003**, *15*, 2854-2860.
7. Mora-Sero, I.; Gimenez, S.; Fabregat-Santiago, F.; Gomez, R.; Shen, Q.; Toyoda, T.; Bisquert, J. Recombination in Quantum Dot Sensitized Solar Cells. *Acc. Chem. Res.***2009**, *42*, 1848-1857.
8. Hossain, M. A.; Jennings, J. R.; Koh, Z. Y.; Wang, Q. Carrier Generation and Collection in Cds/Cdse-Sensitized Sno2 Solar Cells Exhibiting Unprecedented Photocurrent Densities. *Acs Nano* **2011**, *5*, 3172-3181.
9. Peter, L. M.; Riley, D. J.; Tull, E. J.; Wijayantha, K. G. U. Photosensitization of Nanocrystalline TiO_2 by Self-Assembled Layers of Cds Quantum Dots. *Chem. Commun.* **2002**, 10, 1030-1031.
10. Yella, A.; Lee, H. W.; Tsao, H. N.; Yi, C. Y.; Chandiran, A. K.; Nazeeruddin, M. K.; Diau, E. W. G.; Yeh, C. Y.; Zakeeruddin, S. M.; Gratzel, M. Porphyrin-Sensitized Solar Cells with Cobalt (II/III)-Based Redox Electrolyte Exceed 12 Percent Efficiency. *Science* **2011**, *334*, 629-634.
11. Pan, Z. X.; Mora-Sero, I.; Shen, Q.; Zhang, H.; Li, Y.; Zhao, K.; Wang, J.; Zhong, X. H.; Bisquert, J. High-Efficiency "Green" Quantum Dot Solar Cells. *J. Am. Chem. Soc.* **2014**, *136*, 9203-9210.
12. Liu, M. N.; Wang, H. X.; Yan, C.; Will, G.; Bell, J. One-Step Synthesis of Titanium Oxide with Trilayer Structure for Dye-Sensitized Solar Cells. *Appl. Phys. Lett.* **2011**, *98*, 133113.
13. Wang, H. X.; Liu, M. N.; Yan, C.; Bell, J. Reduced Electron Recombination of Dye-Sensitized Solar Cells Based on TiO_2 Spheres Consisting of Ultrathin Nanosheets with 001 Facet Exposed. *Beilstein J. Nanotech.* **2012**, *3*, 378-387.
14. Wang, H. X.; Liu, M. N.; Zhang, M.; Wang, P.; Miura, H.; Cheng, Y.; Bell, J. Kinetics of Electron Recombination of Dye-Sensitized Solar Cells Based on TiO_2 Nanorod Arrays Sensitized with Different Dyes. *Phys. Chem. Chem. Phys.* **2011**, *13*, 17359-17366.
15. Hodes, G. Comparison of Dye- and Semiconductor-Sensitized Porous Nanocrystalline Liquid Junction Solar Cells. *J. Phys. Chem. C* **2008**, *112*, 17778-17787.
16. Kamat, P. V. Boosting the Efficiency of Quantum Dot Sensitized Solar Cells through Modulation of Interfacial Charge Transfer. *Acc. Chem. Res.* **2012**, *45*, 1906-1915.
17. Gonzalez-Pedro, V.; Xu, X. Q.; Mora-Sero, I.; Bisquert, J. Modeling High-Efficiency Quantum Dot Sensitized Solar Cells. *Acs Nano* **2010**, *4*, 5783-5790.
18. Zewdu, T.; Clifford, J. N.; Hernandez, J. P.; Palomares, E. Photo-Induced Charge Transfer Dynamics in Efficient TiO_2/CdS/CdSe Sensitized Solar Cells. *Energy Environ. Sci.* **2011**, *4*, 4633-4638.

19. Zhu, H. M.; Song, N. H.; Lian, T. Q. Charging of Quantum Dots by Sulfide Redox Electrolytes Reduces Electron Injection Efficiency in Quantum Dot Sensitized Solar Cells. *J. Am.Chem. Soc.* **2013**, *135*, 11461-11464.
20. Ahmed, R.; Will, G.; Bell, J.; Wang, H. X. Size-Dependent Photodegradation of CdS Particles Deposited onto TiO_2 Mesoporous Films by Silar Method. *J. Nanoparticle Res.* **2012**, *14*, 1140.
21. Shen, Q.; Kobayashi, J.; Diguna, L. J.; Toyoda, T. Effect of ZnS Coating on the Photovoltaic Properties of CdSe Quantum Dot-Sensitized Solar Cells. *J. Appl. Phys.* **2008**, *103*. 084304.
22. Zhu, H. M.; Song, N. H.; Lian, T. Q. Controlling Charge Separation and Recombination Rates in CdSe/ZnS Type I Core-Shell Quantum Dots by Shell Thicknesses. *J. Am. Chem.Soc.* **2010**, *132*, 15038-15045.
23. Chang, J. Y.; Su, L. F.; Li, C. H.; Chang, C. C.; Lin, J. M. Efficient "Green" Quantum Dot-Sensitized Solar Cells Based on Cu_2S-$CuInS_2$-ZnSe Architecture. *Chem.Commun.* **2012**, *48*, 4848-4850.
24. Yan, K. Y.; Zhang, L. X.; Qiu, J. H.; Qiu, Y. C.; Zhu, Z. L.; Wang, J. N.; Yang, S. H. A Quasi-Quantum Well Sensitized Solar Cell with Accelerated Charge Separation and Collection. *J. Am. Chem. Soc.* **2013**, *135*, 9531-9539.
25. Boldt, K.; Schwarz, K. N.; Kirkwood, N.; Smith, T. A.; Mulvaney, P. Electronic Structure Engineering in ZnSe/CdS Type-II Nanoparticles by Interface Alloying. *J. Phys. Chem. C* **2014**, *118*, 13276-13284.
26. Soni, U.; Pal, A.; Singh, S.; Mittal, M.; Yadav, S.; Elangovan, R.; Sapra, S. Simultaneous Type-I/Type-II Emission from CdSe/CdS/ZnSe Nano-Heterostructures. *Acs Nano* **2014**, *8*, 113-123.
27. Ivanov, S. A.; Achermann, M. Spectral and Dynamic Properties of Excitons and Biexcitons in Type-II Semiconductor Nanocrystals. *Acs Nano* **2010**, *4*, 5994-6000.
28. Verma, S.; Kaniyankandy, S.; Ghosh, H. N., Charge Separation by Indirect Bandgap Transitions in CdS/ZnSe Type-II Core/Shell Quantum Dots. *J. Phys.Chem. C* **2013**, *117*, 10901-10908.
29. Wang, H. X.; Peter, L. M. Influence of Electrolyte Cations on Electron Transport and Electron Transfer in Dye-Sensitized Solar Cells. *J. Phys. Chem. C* **2012**, *116*, 10468-10475.
30. Cameron, P. J.; Peter, L. M. Characterization of Titanium Dioxide Blocking Layers in Dye-Sensitized Nanocrystalline Solar Cells. *J. Phys. Chem. B* **2003**, *107*, 14394-14400.
31. Ahmed, R.; Will, G.; Bell, J.; Wang, H. Size-Dependent Photodegradation of CdS Particles Deposited onto TiO_2 Mesoporous Films by Silar Method. *J. Nanoparticle Res.* **2012**, *14*, 1140.
32. Lee, H.; Wang, M.; Chen, P.; Gamelin, D.; Zakeeruddin, S.; Grätzel, M.; Nazeeruddin, M. Efficient Cdse Quantum Dot-Sensitized Solar Cells Prepared by an Improved Successive Ionic Layer Adsorption and Reaction Process. *Nano Letters* **2009**, *9*, 4221-4227.
33. Nakade, S.; Kanzaki, T.; Wada, Y.; Yanagida, S., Stepped Light-Induced Transient Measurements of Photocurrent and Voltage in Dye-Sensitized Solar Cells: Application for Highly Viscous Electrolyte Systems. *Langmuir* **2005**, *21*, 10803-10807.
34. Duffy, N. W.; Peter, L. M.; Rajapakse, R. M. G.; Wijayantha, K. G. U. A Novel Charge Extraction Method for the Study of Electron Transport and Interfacial Transfer in Dye Sensitised Nanocrystalline Solar Cells. *Electrochem. Commun.* **2000**, *2*, 658-662.

35. Peng, Z. Y.; Liu, Y. L.; Zhao, Y. H.; Chen, K. Q.; Cheng, Y. Q.; Kovalev, V.; Chen, W. ZnSe Passivation Layer for the Efficiency Enhancement of $CuInS_2$ Quantum Dots Sensitized Solar Cells. *J. Alloys & Compounds* **2014**, *587*, 613-617.
36. Tian, J. J.; Zhang, Q. F.; Uchaker, E.; Gao, R.; Qu, X. H.; Zhang, S. E.; Cao, G. Z. Architectured ZnO Photoelectrode for High Efficiency Quantum Dot Sensitized Solar Cells. *Energy & Environ. Sci.* **2013**, *6*, 3542-3547.
37. Barnes, P. R. F.; Anderson, A. Y.; Koops, S. E.; Durrant, J. R.; O'Regan, B. C. Electron Injection Efficiency and Diffusion Length in Dye-Sensitized Solar Cells Derived from Incident Photon Conversion Efficiency Measurements. *J. Phys.Chem. C* **2009**, *113*, 1126-1136.
38. Villanueva-Cab, J.; Wang, H. X.; Oskam, G.; Peter, L. M. Electron Diffusion and Back Reaction in Dye-Sensitized Solar Cells: The Effect of Nonlinear Recombination Kinetics. *J. Phys. Chem. Lett.* **2010**, *1*, 748-751.
39. Dabbousi, B. O.; RodriguezViejo, J.; Mikulec, F. V.; Heine, J. R.; Mattoussi, H.; Ober, R.; Jensen, K. F.; Bawendi, M. G. (CdSe)ZnS Core-Shell Quantum Dots: Synthesis and Characterization of a Size Series of Highly Luminescent Nanocrystallites. *J.Phys. Chem. B* **1997**, *101*, 9463-9475.
40. Sambur, J. B.; Parkinson, B. A. CdSe/ZnS Core/Shell Quantum Dot Sensitization of Low Index TiO_2 Single Crystal Surfaces. *J. Am. Chem. Soc.* **2010**, *132*, 2130-2131.
41. Gratzel, M. Recent Advances in Sensitized Mesoscopic Solar Cells. *Acc. Chem. Res.* **2009**, *42*, 1788-1798.
42. Nguyen, T. T. O.; Peter, L. M.; Wang, H. X. Characterization of Electron Trapping in Dye-Sensitized Solar Cells by near-IR Transmittance Measurements. *J. Phys.Chem.C* **2009**, *113*, 8532-8536.
43. Wang, H. X.; Peter, L. A. A Comparison of Different Methods to Determine the Electron Diffusion Length in Dye-Sensitized Solar Cells. *J. Phys. Chem. C* **2009**, *113*, 18125-18133.
44. Bisquert, J.; Vikhrenko, V. S. Interpretation of the Time Constants Measured by Kinetic Techniques in Nanostructured Semiconductor Electrodes and Dye-Sensitized Solar Cells. *J. Phys.Chem. B* **2004**, *108*, 2313-2322.
45. Zhu, H. M.; Song, N. H.; Lian, T. Q. Wave Function Engineering for Ultrafast Charge Separation and Slow Charge Recombination in Type II Core/Shell Quantum Dots. *J. Am. Chem. Soc.* **2011**, *133*, 8762-8771.
46. Guijarro, N.; Lana-Villarreal, T.; Mora-Sero, I.; Bisquert, J.; Gomez, R. CdSe Quantum Dot-Sensitized TiO_2 Electrodes: Effect of Quantum Dot Coverage and Mode of Attachment. *J. Phys. Chem. C* **2009**, *113*, 4208-4214.
47. Wang, H.; Liu, M.; Zhang, M.; Wang, P.; Miura, H.; Cheng, Y.; Bell, J. Kinetics of Electron Recombination of Dye-Sensitized Solar Cells Based on TiO_2 Nanorod Arrays Sensitized with Different Dyes. *Phys. Chem. Chem. Phys.* **2011**, *13*, 17359-17366.
48. Barnes, P. R. F.; Miettunen, K.; Li, X. E.; Anderson, A. Y.; Bessho, T.; Gratzel, M.; O'Regan, B. C. Interpretation of Optoelectronic Transient and Charge Extraction Measurements in Dye-Sensitized Solar Cells. *Adv. Mater.* **2013**, *25*, 1881-1922.
49. Nazeeruddin, M. K.; Kay, A.; Rodicio, I.; Humphrybaker, R.; Muller, E.; Liska, P.; Vlachopoulos, N.; Gratzel, M. Conversion of Light to Electricity by Cis-X2bis(2,2'-Bipyridyl-4,4'-Dicarboxylate)Ruthenium(II) Charge-Transfer Sensitizers (X = Cl^-, Br^-, I^-, C^{n-}, and Sc^{n-}) on Nanocrystalline TiO_2 Electrodes. *J. Am. Chem.Soc.* **1993**, *115*, 6382-6390.
50. Kumar, A.; Santangelo, P. G.; Lewis, N. S. Electrolysis of Water at $SrTiO_3$ Photoelectrodes - Distinguishing between the Statistical and Stochastic Formalisms for Electron-

Transfer Processes in Fuel-Forming Photoelectrochemical Systems. *J. Phys. Chem.* **1992**, *96*, 834-842.
51. Daeneke, T.; Mozer, A. J.; Uemura, Y.; Makuta, S.; Fekete, M.; Tachibana, Y.; Koumura, N.; Bach, U.; Spiccia, L. Dye Regeneration Kinetics in Dye-Sensitized Solar Cells. *J. Am. Chem.Soc.* **2012**, *134*, 16925-16928.

Table of Contents